Particle Accelerators, 1986, Vol. 18, pp. 203–213
0031-2460/86/1803–0203/$20.00/0

Printed in the United States of America

BEAM TRAPPING IN HIGH-CURRENT CYCLIC ACCELERATORS WITH STRONG FOCUSING FIELDS

P. SPRANGLE and C. A. KAPETANAKOS

Plasma Physics Division, Naval Research Laboratory, Washington, D.C. 20375-5000

(*Received January 2, 1985; in final form March 25, 1985*)

In this paper we investigate a possible mechanism for trapping an intense relativistic electron beam confined by strong focusing fields. In our model, the electron beam is assumed to be injected off axis, into torsatron fields near the chamber walls. The finite resistivity of the walls results in a drag force on the beam centroid that may cause the beam to spiral inwards towards the axis of the chamber. We have analyzed this mechanism and obtained decay rates for the inward spiraling beam motion.

I. INTRODUCTION

In cyclic induction accelerators[1] such as the conventional[2,3] and the modified betatron,[4–7] the energy of the particles increases slowly in synchronism with the vertical (betatron) magnetic field. For example, the NRL modified betatron[8] has been designed to increase the energy of the gyrating particles by approximately $\frac{1}{3}$ keV per revolution.

As a consequence of the slow acceleration, the charged particles must be confined by the weak focusing magnetic field over long periods of time, typically milliseconds, and thus field errors,[9,10] instabilities[11–15] and radiation losses can impose limitations on the acceleration process. These limitations could be substantially relaxed if the acceleration were to occur rapidly, say over a few microseconds. An appropriate name for such an accelerator is REBA-TRON (Rapid Electron Beam Accelerator).

A possible configuration for a rebatron is shown schematically in Fig. 1. The high-gradient localized electric field, responsible for the rapid acceleration, is produced by a convoluted parallel transmission line,[15] although other transmission lines would also be suitable. Since the acceleration occurs over a few microseconds, the vertical magnetic field cannot be increased in synchronism with the energy of the particles. Therefore a strong focusing field is needed to confine the high-current electron beam.[16–20] The confining properties of torsatron magnetic fields in rebatrons have been studied recently and the results are very promising.[21]

In this paper, we consider a possible mechanism that could trap a high-current electron beam in the strong focusing magnetic fields of the rebatron, and probably also applicable to the Racetrack Induction Accelerator.[22] The beam-trapping process in rebatrons is inherently difficult since the strong focusing fields result in particle orbits that are relatively insensitive to an energy mismatch.[20] Thus small

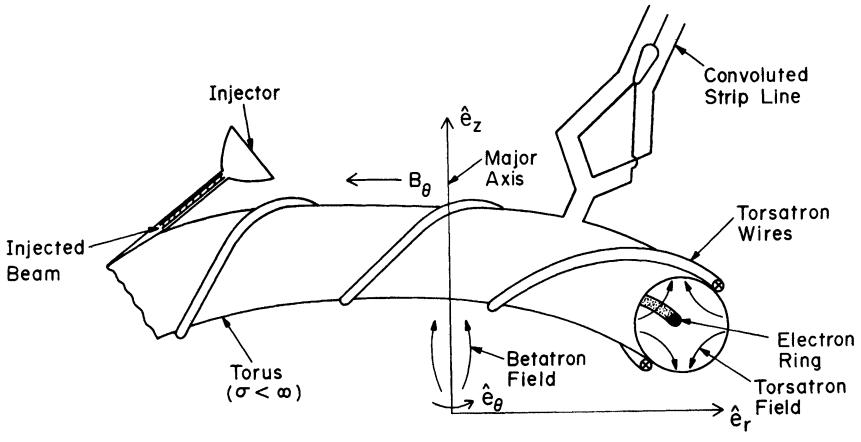

FIGURE 1 Schematic of a rebatron accelerator.

changes in the betatron magnetic field are not sufficient to move the beam from the injection point to the center of the chamber.

The proposed injection scheme is based on the presence of a drag force that acts on the beam centroid when the chamber walls are resistive.[13] Consider a pencil-like electron beam inside a straight, finite-conductivity chamber. In the absence of strong-focusing fields, the image or induced forces, due to the self fields, cause the beam centroid to undergo transverse motion within the chamber. In a perfectly conducting chamber, the induced force **F**, which is directed normal to the chamber wall, and the external longitudinal magnetic field produce a $\mathbf{F}\times\mathbf{B}$ force on the beam. This force causes the beam to execute transverse bounce oscillations within the chamber. However, when the resistivity of the wall is finite, the decay of the wall currents produces a component of induced force directed tangentially to the wall and in the opposite direction to the rotational velocity. For a straight electron beam, this drag force, together with the longitudinal magnetic field, causes the beam to spiral outward towards the chamber walls. For a circular electron beam, the beam centroid spirals inward towards the center of the chamber if $n_s r_b^2/a^2 < \frac{1}{2}$, where n_s is the self-field index, r_b is the beam radius, a is the wall radius and the external field index has been set equal to $\frac{1}{2}$.

In the presence of strong focusing fields, the bounce (poloidal) motion of the beam is due mainly to the gradients of the external magnetic fields and its direction can be selected to provide an inward drift velocity of the beam centroid, resulting in an inward spiraling motion.

The implications of the resistive wall on the stability of the beam must be carefully considered. However, since the relativistic cyclotron frequency corresponding to the vertical field varies rapidly with time, it is likely that longitudinal instabilities and, in particular, the resistive-wall mode can be avoided.

To determine how rapidly the beam can be moved from the wall to the axis of the chamber, we have analyzed the beam dynamics inside a straight cylindrical pipe having resistive walls. Our analysis indicates that for a fairly wide range of parameters, the beam centroid can spiral inward from its injection position, near the wall of the chamber, to the axis of the chamber in less than 50 nanoseconds.

II. DYNAMICS OF THE BEAM CENTROID

To make the problems analytically tractable, the dynamics of the beam is studied in cylindrical geometry, i.e., toroidal corrections associated with the fields are neglected.

Consider a pencil-like electron beam inside a straight cylindrical pipe of circular cross section, as shown in Fig. 2. The pipe thickness is denoted by $\Delta = b - a$, where a is the inner and b the outer radius; σ is the wall conductivity. The centroid of the beam is located at the coordinates (x, y) relative to the center of the minor cross section of the chamber.

The transverse components of the torsatron fields or rotating-quadrupole magnetic field near the z-axis are of the form

$$b_x = b_0 k_w (y \cos k_w z - x \sin k_w z), \tag{1a}$$

$$b_y = b_0 k_w (x \cos k_w z + y \sin k_w z), \tag{1b}$$

where $k_w = 2\pi/l$, l is the period of the magnetic field and b_0 is a constant that is a measure of the field strength. In addition to the external transverse periodic field in Eq. (1), we also have a constant uniform axial magnetic field given by $\mathbf{B}_0 = B_0 e_z$, which is the sum of the torsatron axial field and any additional external axial magnetic field. The induced electric field due to image charges on the walls of the conducting chamber is not affected by the finite wall conductivity and is given by

$$\mathbf{E}_{\text{ind}} = \frac{-2m_0c^2}{|e|}\frac{\nu}{a^2}(x(t)e_x + y(t)e_y), \tag{2}$$

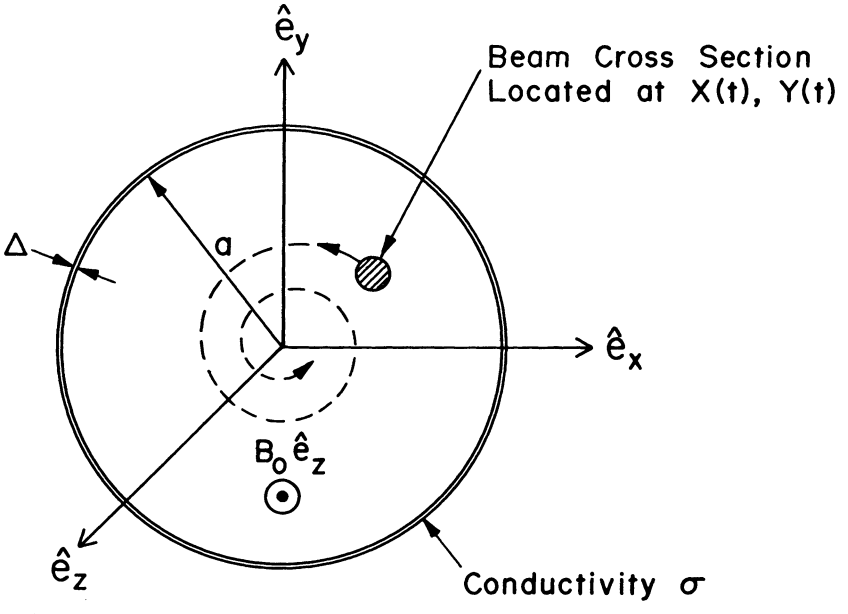

FIGURE 2 Model of cross section of rebatron chamber showing the transverse location of the electron beam. The beam transverse dynamics is influenced by the torsatron field, axial magnetic field and induced fields.

where a is the radius of the chamber, m_0 is the electron mass, c is the velocity of light, $|e|$ is the magnitude of the electronic charge, and ν is Budker's parameter. This parameter can be expressed as $\nu = (\omega_b r_b/2c)^2$, where $\omega_b = (4\pi |e|^2 n_0/m_0)^{1/2}$ is the electron-beam plasma frequency, n_0 is the electron beam density and r_b is the beam radius. The induced magnetic field at the center of the beam is due to image currents flowing in the finite conductivity wall. This magnetic field is modified by the finite wall conductivity and can be written in the form

$$\mathbf{B}_{\text{ind}} = \frac{2m_0c^2}{|e|}\frac{\nu}{a^2}\beta_0 \int_0^t G(t-\tau)(y(\tau)e_x - x(\tau)e_y)\, d\tau, \tag{3}$$

where $\beta_0 = v_0/c$, v_0 is the constant axial beam velocity and $G(t-\tau)$ is the magnetic diffusion function. The induced magnetic field in Eq. (3), in the form of a convolution integral, denotes the fact that the field is a nonlocal function of time. The function $G(t-\tau)$ has been derived elsewhere[13] and we will simply state it when needed. For infinitely conducting walls $G(t-\tau) \to \delta(t-\tau)$ and the induced magnetic field in Eq. (3) reduces to its usual form.

The transverse velocity of the beam centroid is nonrelativistic, i.e., $|\dot{x}|, |\dot{y}| \ll c$, whereas the axial beam particle velocity is highly relativistic and is assumed constant. Using the external field in Eq. (1) and the induced fields given in Eqs. (2) and (3), together with the external solenoidal field $B_0 e_z$, the equations governing the transverse motion of the beam centroid are

$$\ddot{x}(t) - \omega_s^2 x(t) + \Omega_0 \dot{y}(t) - \omega_0\omega_w[x(t)\cos\omega_w t + y(t)\sin\omega_w t] = -\omega_s^2\gamma_0^2\beta_0^2 \int_0^t \delta G(t-\tau)x(\tau)\, d\tau, \tag{4a}$$

$$\ddot{y}(t) - \omega_s^2 y(t) - \Omega_0 \dot{x}(t) + \omega_0\omega_w[y(t)\cos\omega_w t - x(t)\sin\omega_w t] = -\omega_s^2\gamma_0^2\beta_0^2 \int_0^t \delta G(t-\tau)y(\tau)\, d\tau, \tag{4b}$$

where $\omega_s^2 = 2c^2\nu/(\gamma_0^3 a^2)$, $\Omega_0 = |e|\, B_0/(\gamma_0 m_0 c)$, $\omega_0 = |e|\, b_0/(\gamma_0 m_0 c)$, $\omega_w = k_w v_0$, $\gamma_0 = (1-\beta_0^2)^{-1/2}$ and $\delta G(t-\tau) = G(t-\tau) - \delta(t-\tau)$. The right hand side of Eqs. (4a, b) contains the finite wall conductivity effects and vanishes for perfectly conducting walls. In obtaining Eqs. (4a, b) we have set $z = v_0 t$ in Eqs. (1a, b) since we are seeking the time evolution of a cross section of the beam centroid. Rather than solving Eqs. (4a, b) directly, it has been found convenient to first transform these equations to a frame rotating with a frequency $\omega_w/2$ about the z-axis. The transformation that rotates the beam centroid coordinates in these two frames is

$$x(t) = x'(t)\cos(\omega_w t/2) - y'(t)\sin(\omega_w t/2), \tag{6a}$$

$$y(t) = x'(t)\sin(\omega_w t/2) + y'(t)\cos(\omega_w t/2), \tag{6b}$$

where $x'(t)$ and $y'(t)$ are the coordinates of the beam centroid in the rotating frame.

Substituting Eqs. (6a, b) into Eqs. (4a, b) and rearranging terms, we find that

the macroscopic beam motion in the rotating frame is given by

$$\ddot{x}'(t)+\Omega_x^2 x'(t)+(\Omega_0-w_\omega)\dot{y}'(t)$$
$$=-\omega_s^2\gamma_0^2\beta_0^2\int_0^t \delta G(t-\tau)[x'(\tau)\cos\omega_w(t-\tau)/2+y'(\tau)\sin\omega_w(t-\tau)/2]\,d\tau, \quad (7a)$$

$$\ddot{y}'(t)+\Omega_y^2 y'(t)-(\Omega_0-\omega_w)\dot{x}'(t)$$
$$=-\omega_s^2\gamma_0^2\beta_0^2\int_0^t \delta G(t-\tau)[y'(\tau)\cos\omega_w(t-\tau)/2-x'(\tau)\sin\omega_w(t-\tau)/2]\,d\tau, \quad (7b)$$

where

$$\Omega_{\substack{x\\y}}^2=(\Omega_0-\omega_w/2)\omega_w/2-\omega_s^2\mp\omega_0\omega_w.$$

Dropping the primes on x and y and taking the Laplace transform of Eqs. (7a, b) we find that

$$\tilde{x}(s)=F_x(s,\,t=0)/D(s), \quad (8a)$$

$$\tilde{y}(s)=F_y(s,\,t=0)/D(s), \quad (8b)$$

where $\tilde{x}(s)$, $\tilde{y}(s)$ are the transforms of $x(t)$ and $y(t)$ respectively,

$$D(s)=(s^2+\Omega_x^2+\omega_s^2\gamma_0^2\beta_0^2\delta\tilde{C}(s)][(s^2+\Omega_y^2+\omega_s^2\gamma_0^2\beta_0^2\delta\tilde{C}(s))$$
$$+((\Omega_0-\omega_w)s+\omega_s^2\gamma_0^2\beta_0^2\delta\tilde{S}(s))^2 \quad (9a)$$

and

$$\delta\tilde{C}(s)=\tfrac{1}{2}(\delta G(s-i\omega_w/2)+\delta G(s+i\omega_w/2)), \quad (9b)$$

$$\delta\tilde{S}(s)=\frac{1}{2i}(\delta G(s-i\omega_w/2)-\delta G(s+i\omega_w/2)), \quad (9c)$$

are the transforms of $\delta G(t)\cos(\omega_w t/2)$ and $\delta G(t)\sin(\omega_w t/2)$ respectively.

The initial conditions on x, y, $\dot{x}$ and $\dot{y}$ are contained within the functions $F_x(s,\,t=0)$ and $F_y(s,\,t=0)$. The exact forms of these functions are not of interest since we will be mainly concerned with the roots of the function $D(s)$, which is independent of initial conditions.

For an infinitely conducting chamber, i.e., when $\sigma=\infty$, the functions $\delta\tilde{C}(s)=\delta\tilde{S}(s)$ vanish and $D(s)|_{\sigma=\infty}\equiv D_\infty(s)$ becomes

$$D_\infty(s)=(s^2+\Omega_x^2)(s^2+\Omega_y^2)+s^2(\Omega_0-\omega_w)^2. \quad (10)$$

The roots of $D_\infty(s)=0$, which will be denoted by s_0, determine the characteristic frequencies associated with the beam centroid motion and are given by

$$s_0^2=-\frac{(\Omega_x^2+\Omega_y^2+(\Omega_0-\omega_w)^2)}{2}\pm\tfrac{1}{2}((\Omega_x^2+\Omega_y^2+(\Omega_0-\omega_w)^2)^2-4\Omega_x^2\Omega_y^2)^{1/2}. \quad (11)$$

Performing a Taylor expansion about $s=s_0$ we find that the roots of $D(s)=0$ in Eq. (9) are given by

$$s=s_0-\frac{D(s_0)}{\partial D(s)/\partial s|_{s=s_0}}, \quad (12)$$

where s_0 is given in Eq. (11),

$$D(s_0) = 2\omega_s^2\gamma_0^2\beta_0^2\left[\left(s_0^2+\frac{\Omega_x^2+\Omega_y^2}{2}\right)\delta C(s_0)+(\Omega_0-\omega_w)s_0\delta S(s_0)\right], \tag{13a}$$

and

$$\left.\frac{\partial D(s)}{\partial s}\right|_{s=s_0} \approx 4s_0(s_0^2+(\Omega_x^2+\Omega_y^2+(\Omega_0-\omega_w)^2)/2). \tag{13b}$$

Substituting Eqs. (13a, b), together with Eqs. (9b, c), into Eq. (12) yields

$$s = s_0 - \frac{\omega_s^2\gamma_0^2\beta_0^2[\Omega_+^2(s_0)\delta G(s_0+i\omega_w/2)+\Omega_-^2(s_0)\delta G(s_0-i\omega_w/2)]}{4s_0[s_0^2+(\Omega_x^2+\Omega_y^2+(\Omega_0-\omega_w)^2)/2]}, \tag{14a}$$

where

$$\Omega_\pm^2(s_0) = s_0^2+(\Omega_x^2+\Omega_y^2)/2 \pm is_0(\Omega_0-\omega_w). \tag{14b}$$

As mentioned earlier, the derivation of the Laplace transform of the diffusion term, $\delta G(s) = G(s)-1$ will not be repeated here. It has been derived elsewhere[13] and found to be given by

$$\delta G(s) = 2/(F(s)-1), \tag{15a}$$

where

$$F(s) = -\frac{a}{\Delta}\mu(s)\frac{\left[1+\frac{b}{\Delta}\mu(s)\tanh\mu(s)\right]}{\left[\tanh\mu(s)+\frac{b}{\Delta}\mu(s)\right]}, \tag{15b}$$

and

$$\mu(s) = \Delta(4\pi\sigma s/c^2+1/a^2)^{1/2}. \tag{15c}$$

Equation (14) together with Eq. (15) completes the formal derivation of the roots of $D(s) = 0$, which in turn determine the dynamics of the beam centroid within the resistive chamber.

The real part of s determines the macroscopic motion of the beam. If $\mathrm{Re}\,(s) < 0$, the beam centroid spirals inward towards the center of the chamber. If $\mathrm{Re}\,(s) > 0$, the beam is unstable and its centroid spirals outward, away from the center of the chamber. To utilize this mechanism for trapping the beam, it is required that $\mathrm{Re}\,(s) < 0$ and that the magnitude of $\mathrm{Re}\,(s)$ be sufficiently large for the beam to spiral to the center of the chamber in a reasonably short period of time.

III. GROWTH RATE IN THE ABSENCE OF TORSATRON FIELDS

We first consider the trivial case where the torsatron magnetic field vanishes, i.e., $\omega_0 = 0$. In the absence of the strong focusing field, it is unnecessary to transform

to the rotating frame; hence we also take $\omega_w = 0$. For $\omega_s^2/\Omega_0^2 \ll 1$, we find that

$$s = s_0 + \frac{\omega_s^4 \gamma_0^2 \beta_0^2 \delta G(s_0)}{s_0 \Omega_0^2}, \tag{16}$$

where the slow mode is $s_0 = i\omega_B$ and $\omega_B = \pm \omega_s^2/|\Omega_0|$. The fast mode has been neglected because its contribution to the growth rate is much smaller than the contribution from the slow mode. The real part of s is given by

$$\mathrm{Re}\,(s) = \Gamma = \frac{\omega_s^4 \gamma_0^2 \beta_0^2}{\omega_B \Omega_0^2} \mathrm{Im}\,\delta G(i\omega_B), \tag{17}$$

where δG is given by Eq. (15).

When the chamber thickness Δ is much greater than the skin depth associated with the beam-centroid bounce frequency, i.e., $\Delta/\delta_B \gg 1$, we find that

$$\delta G(s_0 = i\omega_B = \pm i\omega_s^2/\Omega_0) = -2^{1/2} \frac{\delta_B}{a} \left(\cos \pi/4 - i \frac{\omega_b}{|\omega_b|} \sin \pi/4 \right), \tag{18}$$

where $\delta_B = c/(2\pi\sigma\,|\,\omega_B|)^{1/2}$ is the skin depth. Substituting Eq. (18) into (17) yields

$$\Gamma = \frac{\omega_s^2 \gamma_0^2 \beta_0^2}{|\Omega_0|} \frac{\delta_B}{a} = 2 \frac{\nu}{\gamma_0} \left(\frac{c}{a} \right)^2 \frac{\beta_0^2}{|\Omega_0|} \frac{\delta_B}{a} > 0, \tag{19}$$

which always results in instability.

IV. DECAY RATE IN THE PRESENCE OF TORSATRON FIELDS

In the presence of the strong focusing field, i.e., when $\omega_0 \neq 0$, we may neglect the self-field contribution, i.e., ω_s^2, in the evaluation of the characteristic frequencies of the macroscopic beam motion.

Using the definitions

$$\varepsilon_w = \omega_w/\Omega_0, \tag{20a}$$

and

$$\varepsilon_0 = 2\omega_0/\Omega_0 = 2b_0/B_0, \tag{20b}$$

and assuming ε_w^2, $\varepsilon_0^2 \ll 1$, we find that the characteristic frequencies given by Eq. (11) are

$$s_0^2 = -\Omega_0^2 \begin{cases} \dfrac{\varepsilon_w^2}{4}(1 - \varepsilon_0^2), & \text{slow} \\ \left(1 - \dfrac{\varepsilon_w}{2}\right)^2 + \dfrac{\varepsilon_w^2 \varepsilon_0^2}{4}, & \text{fast.} \end{cases} \tag{21}$$

Since ε_w^2, $\varepsilon_0^2 \ll 1$, the upper sign in Eq. (11) represents the slow drift motion of the beam centroid and the lower sign denotes the fast motion. In what follows, only the slow macroscopic beam motion will be considered because we are primarily interested in beam trapping.

From Eq. (21), the roots of $D(s)|_{\sigma=\infty}=0$ corresponding to the slow beam motion are given by $s_0 = i\omega_B$, where

$$\omega_B = \pm\Omega_0\varepsilon_w(1-\varepsilon_0^2/2)/2, \tag{22}$$

is the bounce frequency. Since $\varepsilon_0^2 \ll 1$, the bounce frequency in the rotating frame is approximately $\omega_w/2$.

For $\omega_B > 0$, the roots of $D(s)=0$, given in Eq. (14a), become

$$s = i\omega_B + \frac{i\omega_s^2\gamma_0^2\beta_0^2[\Omega_+^2(i\omega_B)\delta G(i(\omega_B+\omega_w/2))+\Omega_-^2(i\omega_B)\delta G(i(\omega_B-\omega_w/2))]}{2\omega_B[\Omega_0^2(1-\varepsilon_w(1-\varepsilon_w/2))-2\omega_B^2]}, \tag{23}$$

where

$$\Omega_\pm^2(i\omega_B) = \Omega_0^2\varepsilon_w \begin{cases} \varepsilon_0^2/4 \\ 1-\varepsilon_w-\varepsilon_0^2(1-2\varepsilon_w)/4. \end{cases} \tag{24}$$

It should be noted that the real part of s is independent of the sign of ω_B. To evaluate the real part of s in Eq. (23), we require the imaginary part of $\delta G(i(\omega_B \pm \omega_B/2))$, where δG is given by Eq. (15). Using Eq. (15c), it is found that

$$\mu(i(\omega_B \pm \omega_w/2)) = \frac{\Delta}{\delta}\begin{cases}(2i(1-\varepsilon_0^2/4))^{1/2} \\ (-i\varepsilon_0^2/2)^{1/2}\end{cases} \tag{25}$$

where

$$\delta = c(2\pi\sigma\,|\omega_w|)^{-1/2} \tag{26}$$

is the skin depth associated with the frequency $\omega_w = v_0 k_w$.

Case (i), $\Delta/\delta \ll 1$

For $\Delta/\delta \ll 1$, δG is given by

$$\delta G(i(\omega_B \pm \omega_w/2)) = \begin{cases} -(1+i(1-\varepsilon_0^2/4)\xi)^{-1} \\ -(1-i\varepsilon_0^2\xi/4))^{-1} \end{cases} \tag{27}$$

and the decay rate becomes

$$\Gamma = \mathrm{Re}\,(s) = \frac{\Omega_0\varepsilon_w\xi}{2\varepsilon_B(1-\varepsilon_w)}(\varepsilon_s\varepsilon_0\gamma_0\beta_0)^2\left(\frac{(1-\varepsilon_w)/4}{1+(\varepsilon_0/2)^4\xi^2}-\frac{1}{1+\xi^2}\right), \tag{28}$$

where $\xi = a\Delta/\delta^2$, $\varepsilon_s = \omega_s/\Omega_0$, $\varepsilon_B = \omega_B/\Omega_0$, ε_s^2, $\varepsilon_B^2 \ll 1$ and $\Delta/\delta \ll 1$.

Case (ii) $(\Delta/\delta)\varepsilon_0/\sqrt{2} \gg 1$

For this case δG is given by

$$\delta G(i(\omega_B \pm \omega_w/2)) = -\sqrt{2}\frac{\delta}{a}\begin{cases}(i)^{-1/2} \\ 2(-i)^{-1/2}/\varepsilon_0\end{cases}, \tag{29}$$

and the decay rate becomes

$$\Gamma = \mathrm{Re}\,(s) = \frac{(\delta/a)\Omega_0\varepsilon_w}{2\varepsilon_B(1-\varepsilon_w)}(\varepsilon_s\varepsilon_0\gamma_0\beta_0)^2\left(\frac{2(1-\varepsilon_w)}{\varepsilon_0^3}-1\right). \tag{30}$$

In both (28) and (30) we have made the assumption that ε_s^2, ε_w^2, ε_0^2, $\varepsilon_B^2 \ll 1$ and $\gamma_0 \gg 1$.

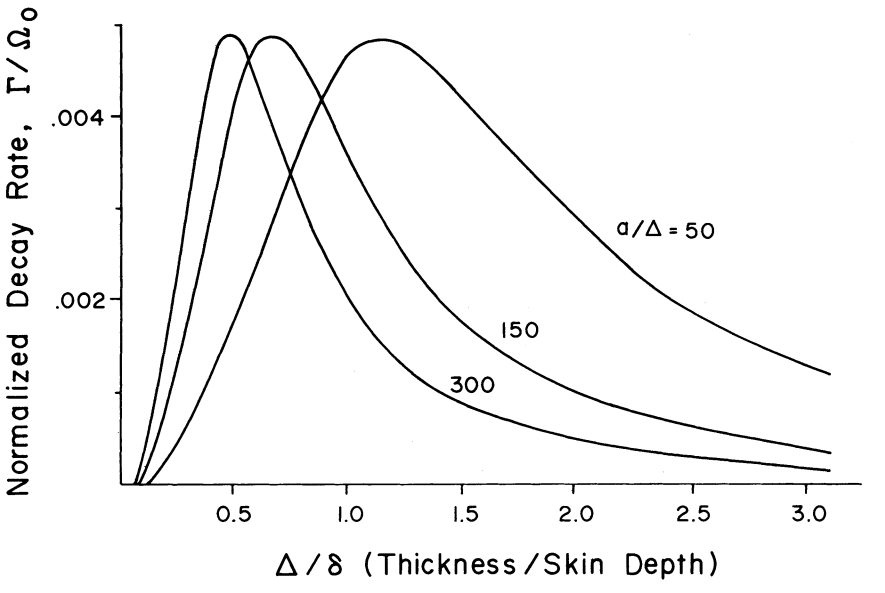

FIGURE 3 Shows the decay rate for the beam centroid as a function of Δ/δ for $a/\Delta = 50$, 150, 300, $\varepsilon_0 = 0.2$, $\varepsilon_w = 0.25$, $\varepsilon_s = 0.02$ and $\gamma_0 = 5$.

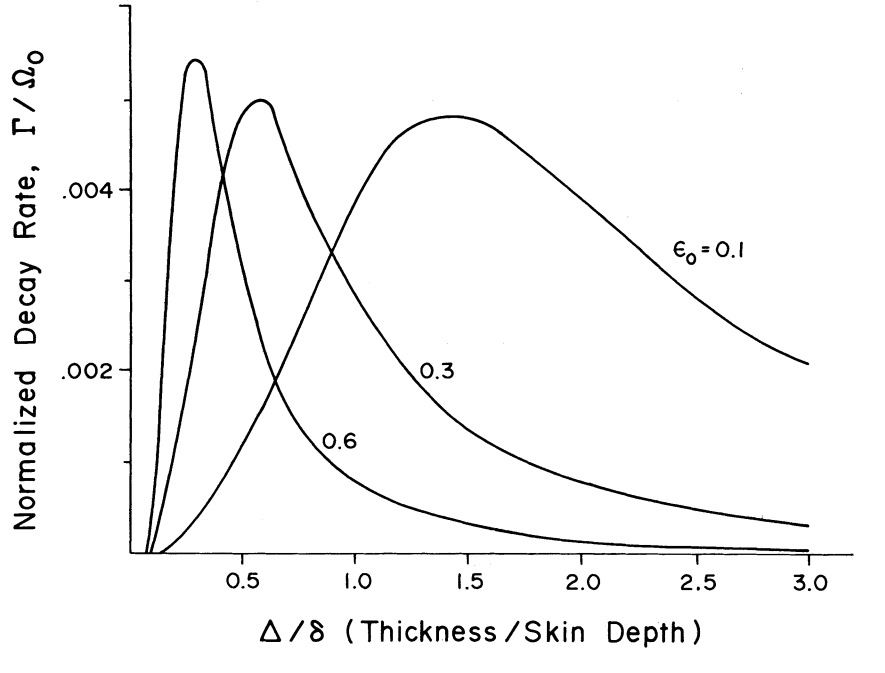

FIGURE 4 Shows the decay rate for the beam centroid as a function of Δ/δ for $\varepsilon_0 = 0.1$, 0.3, 0.6, $a/\Delta = 100$, $\varepsilon_w = 0.25$, $\varepsilon_s = 0.02$ and $\gamma_0 = 5$.

The decay rates given by (14) together with (15) are shown in Figs. (3) and (4) for various sets of parameters.

DISCUSSION

In this paper we have investigated a possible mechanism for trapping an intense relativistic electron beam confined by strong focusing fields. In our model the electron beam is assumed to be injected into the torsatron fields off axis, near the chamber walls. The finite resistivity of the walls results in a drag force on the beam centroid which may cause the beam to spiral inward towards the axis of the chamber. We have analyzed this mechanism and obtained decay rates for the inward spiraling motion.

As an illustration of the trapping process, we consider a 15 kA ($\nu = 0.86$), 2 MeV ($\gamma_0 = 5$) electron beam injected near the wall of a 10 cm radius resistive chamber of thickness $\Delta = a/150$. The axial magnetic field is taken to be $B_0 =$ 2.5 kG, the torsatron coefficient b_0 is 250 G and the magnetic period l of the torsatron field is 12.8 cm. With these parameters we find that $\varepsilon_s = 0.02$, $\varepsilon_w = 0.25$, $\varepsilon_0 = 0.2$, $\varepsilon_B = 0.12$ and $\Omega_0 = 8.8 \times 10^9\ \text{sec}^{-1}$. The maximum decay rate for these parameters occurs (See Fig. 4) at $\Delta/\delta = 0.5$ and is $\Gamma \approx 5 \times 10^{-3}\ \Omega_0 = 4.4 \times 10^7\ \text{sec}^{-1}$. The conductivity of the chamber wall is $\sigma = c^2/(2\pi\,|\omega_w|\,\delta^2) = 4 \times 10^{12}\ \text{sec}^{-1}$, $\omega_w = \varepsilon_w \Omega_0 = 2.2 \times 10^9\ \text{sec}^{-1}$ and $\delta = 2\Delta = 0.13$ cm. The e-fold time for the inward spiraling motion of the beam is $\tau_e = 1/\Gamma \approx 22$ nsec, which is sufficiently fast to trap the beam. It should be noted that in this example for $l_w = 12.8$ cm the linearized fields of Eq. (1) are valid only within a small distance from the axis. In practice, the more exact expressions for the fields should be used and the problem addressed numerically.

ACKNOWLEDGMENTS

This work was partially supported by U. S. Army Ballistic Research Laboratory, Aberdeen Proving Grounds, Maryland and partially by the Office of Naval Research. The authors would also like to thank Eric Sprangle for numerically coding and plotting the analytical results in our paper.

REFERENCES

1. C. A. Kapetanakos and P. Sprangle, to be published in *Phys. Today* (1985).
2. D. W. Kerst, *Nature* **157,** 90 (1946).
3. A. I. Pavlovskii *et al.*, *Sov. Phys. Tech. Phys.* **22,** 218 (1977).
4. P. Sprangle and C. A. Kapetanakos, *J. Appl. Phys.* **49,** 1 (1978).
5. N. Rostoker, *Comments on Plasma Physics*, Vol. 6, p. 91 (1980).
6. C. A. Kapetanakos, P. Sprangle, D. P. Chernin, S. J. Marsh and I. Haber, *Phys. Fluids* **26,** 1634 (1983).
7. G. Barak and N. Rostoker, *Phys. Fluids* **26,** 856 (1983).
8. J. Golden *et al.*, *IEEE Trans. on Nuc. Sci.* Vol. NS-30, No. 4, Pt. 1, p. 2114 (1983).

9. D. Chernin and P. Sprangle, *Part. Accel.* **12,** 101 (1982).
10. C. Agritellis, S. J. Marsh and C. A. Kapetanakos, NRL Memo Report No. 5141 (1983) ADA133089.
11. P. Sprangle and D. Chernin, *Part. Accel.* **15,** 35 (1984).
12. P. Sprangle and J. L. Vomvoridis, NRL Memo Report No. 4688 (1984) ADA142822.
13. P. Sprangle and C. A. Kapetanakos, *Part. Accel.* **14,** 15 (1983).
14. W. M. Manheimer, *Part. Accel.* **13,** 209 (1983).
15. M. T. Buttram, "Transmission Lines for Pulsed Power Applications", Sandia Laboratories, Report No. SAND 83-0957 (1983).
16. L. Teng, Argonne Nat. Lab. Report No. ANLAB-55 (1959).
17. G. Salardi *et al.*, *Nucl. Instr. and Methodes* **59,** 152 (1968).
18. R. M. Pearce, *Nucl. Instr. and Methodes* **83,** 101 (1970).
19. R. L. Gluckstern, *Proc. of Linear Accel. Conf.* 245 (1979).
20. C. W. Roberson, A. Mondelli and D. Chernin, *Phys. Rev. Lett.* **50,** 507 (1983).
21. C. A. Kapetanakos, P. Sprangle, S. J. Marsh, C. Agritellis, D. Dialetis and A. Prakash, NRL Memo Report No. 5503 (1985).
22. A. A. Mondelli and C. W. Roberson, *Part. Accel.* **15,** 221 (1984).